

1 **Effect of the compaction parameters on the final structure and properties of** 2 **a press-coated tablet (Tab-in-Tab): experimental and numerical study of the** 3 **influence of core and shell dimensions**

4 Léo Picart ^{a, b}, Vincent Mazel ^{a,*}, Aline Moulin ^b, Pierre Tchoreloff ^a

5 ^a Univ. Bordeaux, CNRS, Arts et Metiers Institute of Technology, Bordeaux INP, INRAE, I2M Bordeaux,
6 F-33400 Talence, France

7 ^b Skyepharma Production SAS, 55 rue du Montmurier, 38070 Saint-Quentin-Fallavier, France

8 * Corresponding author: address: I2M, Univ. Bordeaux, 146 rue Léo Saignat, F-33000 Bordeaux, France
9 ; tel :+33 5 57 57 92 60 ; E-mail address: vincent.mazel@u-bordeaux.fr

10 **Abstract**

11 With increasing interest in chronopharmaceutics, press-coated tablets have become a key technology in
12 the field of modified release drug delivery systems. Although their benefits in terms of drug release have
13 been largely studied, the comprehension of the compaction process of press-coated tablets is yet to
14 complete. Particularly, the effects of geometrical parameters like the ratios between the
15 thickness/diameter of the core and the thickness/diameter of the whole tablet were so far not much
16 considered. Moreover, there is only few studies in the literature about the effect of the press-coating
17 compression on the final structure and properties of the core. The present work consists in a joint
18 experimental and numerical study that aims to assess these points. The study revealed high stress
19 concentrations on the core during compression, causing high permanent deformations of the core,
20 especially when the ratio between the core thickness to the total tablet thickness was high. The
21 mechanical properties of the core tablet were also shown to be impacted: its density and strength were
22 found to decrease before increasing again along the coating-compression. This effect was highlighted to
23 be dependent on the triaxiality of the stress state (i.e. the ratio between the stresses in the different
24 directions), itself depending on the two studied geometrical parameters. As the properties of the core
25 affect the release attributes, ratios between the dimensions of the core and the dimensions of the whole
26 tablet (thickness, diameter) should be taken into account as critical parameters for the manufacture of
27 press-coated tablets.

28

29

30 **1. Introduction**

31

32 Press-coated tablet is a solid dosage form for controlled release that consists of a “core-shell”
33 structure (Foppoli et al., 2017). Although a variety of release profiles may be obtained, in most of the
34 cases , the active ingredient is contained in a core coated with an inactive shell (Jagdale et al., 2014;
35 Kaljević et al., 2016; Sawada et al., 2004; Wu et al., 2007). In this case, the active ingredient can only
36 be released when the shell itself releases the core, allowing a lag-time before the release of the drug
37 (Conte et al., 1993; Fukui et al., 2000). This kind of pharmaceutical drug delivery system is currently
38 produced at an industrial scale and used to treat patients, especially for applications that needs a
39 precise release place like the colon (Maity and Sa, 2016), or that needs a long term release, for
40 example during the night (Lin and Kawashima, 2012). The therapeutic advantages of pulsatile drug
41 delivery have been widely studied (Gandhi et al., 2011; Lin and Kawashima, 2012), demonstrating
42 high added value in the field of healthcare.

43 The specific structure of the press-coated tablets also makes the press-coating process a very
44 particular case of powder compaction. The process begins with the production of the core, and the
45 second step is the manufacture of the shell by compaction of a free powder surrounding the
46 core(Kaljević et al., 2016). In spite of the long use of the technique and the complexity of the
47 phenomena occurring during this process, there is still very few studies concerning the press-coating
48 manufacturing process and its effects on the mechanical resistance and the functional performance of
49 press-coated tablets.

50 A precursor work (Ascani et al., 2019) started a new interest for the mechanical side of press-coating.
51 The attention was drawn on the influence of core and shell mechanical properties, like stiffness and
52 viscoelastic properties. These properties are confirmed to have large effects on the final product
53 attribute like mechanical resistance, coat defects, and density distribution.

54 Another recent following work also provided links between process parameters, formulation
55 parameters and final properties in the case of press-coated tablets (Nguyen et al., 2020). In this
56 study, several parameters were studied like the core and shell materials, core initial density and

57 compression speed. Through a systematic understanding approach, the influence of these
58 parameters on the layer adhesion, lamination tendency and tablet microstructure were studied.
59 Particularly, in the case of Tab-in-Tab tablets (i.e. press-coated tablets), the release profile should be
60 considered as a critical quality attribute and has to be controlled. As this attribute partly depends on
61 the core which contains the active ingredient, it is necessary to understand how and to what extent
62 the coating-compression impacts the core.

63 The present study aims to evaluate the evolution of the core during the coating-compression. Cores
64 recovered from press-coated tablets, manufactured at different pressures, were characterized in
65 dimensions, density and mechanical strength. As the geometry effects are yet not described in the
66 literature, the diameter ratio between the core and the shell was studied, as well as the thickness of
67 the layer above the core (i.e. the distance between the core surface and the shell surface). These
68 parameters may be critical process parameters that were so far not considered in the design of press-
69 coated tablets and should be extensively studied. Finally, FEM numerical simulation, more and more
70 used in the field of pharmaceutical compaction(Cunningham et al., 2004; Diarra et al., 2012; Sinka et
71 al., 2004; Wu et al., 2005), was carried out as a tool to understand the mechanical phenomena
72 occurring during the coating compression.

73

74 **2. Materials and methods**

75

76 2.1. Powders and blend

77 Classical pharmaceutical excipients were used as model products for this study. Two mixtures were
78 used for the compaction of cores. The first was composed of 99% granulated lactose monohydrate
79 (GLac) (Excipress GR150, Armor Pharma, Loudéac, France) and 1% Magnesium Stearate (Partek
80 Mg Lub, Merck, Darmstadt, Germany). The second was composed of 99,5% (w/w) Microcrystalline
81 Cellulose (MCC) (Vivapur 200, JRS Pharma GmbH, Rosenberg, Germany) and 0.5% Magnesium
82 Stearate. The choice of the two products was based on their different mechanical behavior, lactose
83 being generally considered as brittle and MCC as plastic (Roberts and Rowe, 1987). This will make it
84 possible to broaden the applicability of the presented results.

85 The same MCC mix was used for every shell compression. Lactose mix was not used as a shell for
86 two reasons. First, in the case of MCC cores it led to quasi-systematic lamination upon the ejection.
87 Second, in the case of Lactose, it was found impossible to extract the core from the final form without
88 damage.

89 The powders were blended using a Turbula mixer (Wab, Muttenz, Switzerland) at 49rpm during 5
90 minutes and then stored at a constant relative humidity (RH) of 45% until the compaction.

91

92 2.2. Tablet manufacturing

93 2.2.1. *Compaction simulator*

94 All experiments were performed on a compaction simulator Styl'One Evolution (Medelpharm,
95 Beynost, France). This device is a single station instrumented tableting machine. It is equipped with
96 force sensors (accuracy 10 N) on both punches, and the displacements of the punches are monitored
97 using incremental sensors. The die was filled automatically with a gravity flow feeder containing the
98 powder.

99 2.2.2. *Core compression*

100 The cores were manufactured in three sizes with diameters of 6mm; 8mm; 11.28mm respectively,
101 using for each a set of Euro B round flat punches of the selected diameter. Thicknesses of the cores
102 were set to keep a constant Diameter/Thickness ratio of 8/3. Lactose cores were compacted at a
103 pressure of 300MPa and MCC cores were compacted at a pressure of 150MPa. Compression forces
104 were adjusted to get the same pressure for each size. These manufacturing parameters are reported
105 in the Table 1.

106 The core-tablets were let 48h at 45% RH for relaxation before the coating compression.

107 2.2.3. *Coating-compression*

108 All press-coated tablets were manufactured using Euro B round flat punches of 16mm diameter. After
109 first filling, the core was manually placed on the center of the powder bed. A minimal tamping force
110 was applied to place the top of the core at the level of the powder bed, before the second filling and
111 main compression. The configuration of the resulting press-coated tablet is presented in Figure 1.

112 The filling heights were adjusted to have the target thickness of 0.6mm, 1.0mm or 1.8mm for both
113 upper and lower layers after the compression. In the further text, both upper and lower layers will be
114 referred as “layer”, as they have the same thickness.

115 Two series of press-coated tablets were made. The first one used a constant 8mm diameter core with
116 three different layer thicknesses of 0.6mm, 1.0mm and 1.8mm. The second one used three sizes of
117 core, respectively 6mm, 8mm, 11.28mm, while keeping a constant layer thickness of 1.0mm.

118 For each “Core diameter/Layer thickness” set, symmetrical coating-compression was performed at
119 five different compression pressures, respectively 25MPa, 50MPa, 75MPa, 100MPa and 150MPa.

120 As mentioned above, these experiments were performed on two systems. Each system had MCC as
121 shell and the core was MCC for one of them and Lactose for the other.

122 To ensure the reproducibility of the results, four press-coated tablets were made for each “Core
123 diameter/Layer thickness/Pressure” set. The press-coated tablets were let to relax 48h at 45% RH
124 before the characterization.

125 2.3. Characterization

126 2.3.1. Recovery and measurements of the core

127 Right before the coating-compression, the cores were individually measured in diameter and
128 thickness using an ABS Digital Thickness Gauge (Mitutoyo, Japan, accuracy 3µm), and weighted
129 using a precision scale (AT261, Mettler Toledo, Switzerland, accuracy 0.015mg). After press-coating
130 and relaxation, the press-coated tablets were opened applying a scalpel on the side of the tablet to
131 remove a layer, the cores were then recovered manually to keep them intact. This operation was quite
132 easy to perform and the dimensions of the cores were then measured again following the same
133 process.

134 As the tablets were all cylindrical, the density was calculated from the dimensions and mass:

$$135 \quad \rho = \frac{4 \cdot m}{\pi \cdot d^2 \cdot t} \quad (1)$$

136 where m is the mass of the tablet, d its diameter and t its thickness.

137 For a maximum of precision, every recovered core was compared to its own initial dimensions and
138 density.

140 The diametral compression test was performed using a TA.HDplus texture analyzer (Stable
141 microsystems, Surrey, United Kingdom). Compacts were diametrically compressed between two flat
142 surfaces at a constant speed of 0.5 mm. s⁻¹. To be able to compare the strength of tablets with
143 different sizes, the tensile strength of the core was calculated with the following equation (Fell and
144 Newton, 1970):

$$145 \quad \sigma = \frac{2.F}{\pi.D.t} \quad (2)$$

146 where F is the maximum force reached in the test, D is the tablet diameter and t is the tablet
147 thickness.

148 2.4. Numerical modeling

149 Numerical modeling is nowadays increasingly used in the pharmaceutical industry to study the
150 processes. In the case of compaction, the Finite element method is the most widely used
151 (Cunningham et al., 2004; Diarra et al., 2012; Sinka et al., 2004; Wu et al., 2005). It considers the
152 powder as continuous medium which properties are dependent on the relative density. Results
153 published in the literature show good agreement between experimental results and simulation.

154 Finite Elements Modeling Abaqus® software (Dassault Systèmes, Vélizy-Villacoublay, France) was
155 used to undergo numerical simulations of the die compression of press-coated tablets.

156 An axisymmetric modeling was chosen as the geometry, border limits, and loads are all axisymmetric.
157 The dimensions of the core, shell, die and punches were chosen equal to the ones that were used for
158 the experiments. However, a light chamfer (32°x0.6mm) was introduced on the core geometry to
159 prevent excessive element distortion on the edge of the core. It was considered to have an
160 acceptable impact on the results.

161 The MCC core / MCC shell tablet was chosen to be numerically reproduced, so both core and shell
162 were affected with Drucker-Prager-Cap (DPC) model properties of MCC according to previous results
163 and calibration work (Diarra et al., 2013).

164 A different initial relative density was applied to core and shell: 0.862 for the core which corresponds
165 to a compaction under 150MPa and 0.474 for the shell which is the minimum acceptable density for
166 the modeling and corresponds to a tamping pressure around 12MPa.

167 3. Results

168 In the whole following text, the expression “apparent pressure” will be used and refers to the applied
169 axial compression force of the punches divided by their surface. This variable represents the mean
170 axial pressure on the punches at the compression peak. This expression was chosen to differentiate
171 this value from the effective pressure at a particular location of the core tablet (e.g. in the core). As it
172 will be demonstrated below, the effective pressure can be very different from the apparent one.

173 3.1. Influence of the layer thickness

174 In this part, we studied the variations of the core diameter and thickness as a function of the applied
175 apparent pressure and the influence of the layer thickness on these variations. For this purpose, a
176 series of experiments was led with the layer thickness as the variable parameter, only using cores of
177 8mm diameter. By measuring the cores before and after the compression, the diameter, thickness
178 and density variations were obtained. The results are presented in Figure 2.

179 First of all, in every case the core diameters increased and their thickness decreased in a high
180 proportion after the coating-compression (Figure 2.A-B-D-E). These dimension variations are both
181 increasing with the compression pressure. With a diameter variation up to +15% for MCC cores and
182 to +20% for lactose cores and a thickness up to -30% variation, the “flattening-like” effect is
183 perceptible to the naked eye. Secondly, it appeared that these effects were more important when the
184 layer was thin. Thus, a thin layer acts as an aggravating factor, making the cores to achieve
185 significant deformations even at very low apparent pressure levels compared to their initial
186 compression pressure of 150MPa and 300MPa, for MCC and lactose respectively.

187 Afterwards, the density variations depending on the pressure were studied, with the same three
188 layers’ thicknesses. The results are reported in Figure 2.C-F.

189 For the three studied layer thicknesses, the evolution of the density followed the same trend when the
190 compaction pressure increased. First, the density decreased, then after a certain “apparent pressure”,
191 the density increased again. A decrease of the density is something which is normally not observed
192 during the compaction of powders. Such a loss of density can be interpreted as a partial failure of the
193 core within the shell. As the failure is confined in the shell, the core can undergo further compaction at
194 higher apparent pressures. In the case of MCC core, it even makes it possible to reach density levels
195 higher than the initial one.

196 The influence of the layer thickness is also visible on the density curves. The minimum of core
197 density is reached at a higher level of apparent pressure when the thickness of the layer increases.
198 Thus, the density changes can be observed regardless of the layer thickness, but this parameter has
199 a “shifting” role on the apparent pressure axis. For MCC core, the minimum density is obtained for
200 an apparent pressure around 25MPa for a layer thickness of 0.6mm but for layer of 1.8mm, this
201 minimum is reached between 50 and 75 MPa. The same trend can be seen for Lactose cores. It is
202 therefore clear that the layer thickness is an important parameter that strongly affects the stress state
203 inside the core.

204

205 As the density of the core varies along the coating-compression path, it is important to study its
206 mechanical resistance since these properties are strongly linked. The diametrical compression test
207 was applied on the recovered cores to assess their mechanical strength. The results are given in
208 Figure 3. It is worth noting that the MCC cores recovered from 150MPa tablets with 0.6mm layer
209 thickness are not presented on these curves. The reason is that these cores did not break
210 diametrically, but chipped during the test. Thus, the maximal force reached could not be converted in
211 tensile strength and compared with the other values.

212 As a reference, a series of 8mm diameter tablets was manufactured at different pressure levels using
213 simple die compression. The obtained tablets were measured and tested to assess the tableability
214 and the compactibility of the powder (Tye et al., 2005).

215 The strength of the core tablets (Figure 3.A,C) follows the same tendency as the one previously seen
216 for their density, with a minimum reached at a thickness-dependent apparent pressure and then a
217 further increase.

218 On Figure 3.B,D the same values of tensile strength are plotted as a function of the densities of the
219 cores out of press-coated tablets. The compactibility curve, obtained in a simple die compaction, is
220 also plotted as a reference. This comparison shows that the core tablets that lost density at low
221 apparent pressure are less resistant than tablets of the same density obtained by a simple
222 compression, which agrees with the hypothesis of a failure of the core in the early-compression. The
223 strength loss is even more pronounced with the lactose cores, that are reduced to an extremely low

224 resistance after a coating-compression at only 25MPa, despite being compacted at an initial 300MPa
225 pressure.

226 On the contrary, at higher apparent pressures, the cores have a higher tensile strength than the
227 tablets of the same density obtained by a simple compression. This effect does not seem to be
228 strongly dependent on the external layer thickness. It reveals that the loading path obtained during the
229 coating-compression is able to modify the inner structure of the core tablets in a way which is different
230 from the simple die compaction. As a consequence, two tablets of the same density obtained by press
231 coating or by simple die compaction can have different tensile strengths. This point will be further
232 discussed in the discussion part of the manuscript.

233 In the next part, following the same methodology, another geometrical parameter of the press-coated
234 tablet was studied: the ratio between the shell diameter and the core diameter.

235 3.2. Influence of the core-shell diameters ratio

236 To isolate the influence of the ratio between the core and shell diameters, the same experiments
237 series were undergone with fixed shell-diameter and layer thickness parameters, respectively
238 $d=16\text{mm}$ and $t=1.0\text{mm}$. The only varying parameter was the core size, which was chosen at 6mm,
239 8mm, and 11.28mm. As previously, the results are given in relative variations to make the different
240 sizes comparable. They are presented in Figure 4.

241 As previously, there is an increase of the diameter and a decrease of the thickness of the cores when
242 the apparent pressure increases. Nevertheless, compared to the case of the layer thickness, the size
243 of the core seems to have a smaller influence on the relative deformations. Whereas the three layer
244 thicknesses resulted in three well distinct lines for the core dimensions, the three core sizes showed
245 nearly identical relative deformations (Figure 4.A,B,D,E). Even if there is a slight shift, the results are
246 not showing a consistent trend regarding the diameter. For example, at an apparent pressure of
247 150MPa, the medium core diameter of 8mm shows the highest deformations for both MCC and
248 lactose cores. Another example is the evolution of the diameter of the core of 11.28mm. For MCC
249 cores, it seems to be the diameter with the lowest variations but for lactose cores, the result is much
250 more complex. Considering the present results, it is thus difficult to understand exactly the influence
251 of the core diameter on diameter and thickness variations.

252 For the density variations, again the same trend is obtained for all diameters with a decrease of the
253 density followed by an increase after a certain pressure. Nevertheless, contrary to the case of the
254 layer thickness, the core-shell diameters ratio seems to have no influence on the apparent pressure
255 corresponding to the density minimum (Figure 4.C,F). Again, a clear trend is complicated to observe.
256 Nevertheless, the results for the 11.28mm diameter seems different, especially with a higher density
257 for the high apparent pressures for both cores. For lactose cores it seems that at the lowest apparent
258 pressure (25MPa) the density of the core is inversely proportional to the core diameter whereas the
259 opposite results are obtained at the highest apparent pressure (150MPa). This trend is not so clear for
260 MCC cores. So to conclude, it seems that the core diameter can have an influence on the density
261 evolution but the results presented do not make it possible to clearly define the trend.

262 As for the previous series, the tensile strength of the recovered cores was then assessed performing
263 diametral compression tests. The results are presented in Figure 5.A,C depending on the apparent
264 pressure and Figure 5.B,D depending on the density, in which the path of growing apparent pressure
265 is represented by the lines.

266 First of all, a slight difference of density has been measured between the initial MCC cores of different
267 diameters, even if manufactured at the same pressure. To confirm this fact, the experiment was
268 reproduced several times by changing the measuring tools and the powder, but the same result was
269 obtained each time. This trend was not observed for lactose cores. We have for the moment no
270 explanation for the difference between the MCC cores, and more systematic studies are needed to
271 explain this point, but these studies overpass the objectives of the present work. However, this initial
272 difference is considered acceptable as the results rely on the individual variation of density of each
273 core tablet and not on the comparison of the density between cores of different diameters.

274 For all the cores, as it can be seen in the tabletability profile (Figure 5 A and C), there is an initial
275 decrease of the tensile strength followed by an increase when the apparent pressure further
276 increases. Nevertheless, the compactibility graphs (Figure 5 B and D) show very different behavior
277 depending on the core diameter. As seen previously, the 6mm and 8mm cores strengthen to a higher
278 resistance than the usual resistance of tablets obtained by simple compression of the same density.
279 The curves show the opposite behavior for the 11.28mm cores: after the dedensification and loss of
280 resistance in early-compression, the tensile strength stays inferior to the usual level for a simple die
281 compression until the high apparent coating-pressure of 150MPa. Thus, it is clear that the core

282 diameter has an influence on the triaxial stress state that modifies the structure of the core and
283 consequently, on the final properties of the core.

284 The results of this part highlight again the fact that strength of the powder compact is not a bijection of
285 the density, as it is often assumed in the case of a simple die compression. The strength also
286 depends on the loading path that the tablet has undergone, which is affected by the type of
287 compression, and in the case of the press-coating by the core diameter.

288 The triaxiality of the stresses (i.e. the ratio between the stresses in the different directions) will be
289 discussed in the next part with the use of numerical modelling, explaining how the stress states
290 depend on the studied parameters and can cause the previously seen effects.

291

292 **4. Discussions**

293

294 The described changes of the core and the influence of the layer thickness and core diameter during
295 the press-coating manufacturing process indicate different stress states in different regions of the
296 tablet depending on these two parameters. A series of numerical simulations was made to interpret
297 the experimental results and understand their mechanical origin. The numerical simulation of the
298 coating-compression allows to access local variables inside the compact at a given compression
299 pressure, like stress fields in different directions and relative density field in the shell, which are
300 difficult to assess experimentally. It is well known that FEM simulation might not be completely
301 quantitative as some physical phenomena are not taken into account. Nevertheless, it makes it
302 possible to obtain trends and order of magnitude which are useful to compare the different situations.

303

304 4.1. Influence of the layer thickness

305 The modeling was set with a punch force of 10.05kN to simulate a compression with an apparent
306 pressure of 50MPa. The pressure was chosen to avoid excessive mesh deformation during
307 simulation. The simulated stress state in the compact at this pressure is presented in Figure 6 for the
308 three layer thicknesses of the experiments.

309 The material parameters used are known to correctly describe the densification behavior (Diarra et
310 al., 2013). However, no decrease of core density was observed. This reveals that the calibration of
311 the failure line does not describe well the material behavior which is not really surprising as the failure
312 criterion used (Drucker Prager) might not represent accurately the fracture behavior of a powder bed
313 (Mazel et al., 2014). Thus, the results on the core dimensions and densities were not taken into
314 account. We cannot discard an influence of the changes of the core dimensions on the final results.
315 Nevertheless, the changes in dimension of the core are much smaller than the changes occurring in
316 the shell. We can thus reasonably suppose that these should not have a large influence on the stress
317 and density fields in the shell.

318 The results showed that unlike the case of the simple compression (Diarra et al., 2012), the stress
319 distribution is strongly heterogeneous in the press-coated tablet during compression. Indeed, the axial
320 stress (Figure 6.A) is highly concentrated on the core with values that exceed twice the mean axial
321 stress of 50MPa. This stress concentration is explained by the structure of the system: the core which
322 is very stiff with respect to the loose powder exhibits negligible deformation in the early compression,
323 which means that the thickness change induced by the punch displacement is in fact mainly absorbed
324 by the thin thickness of the upper and lower layers. The layer is thus submitted to a very high strain
325 (relative change in thickness). In the band (i.e. on the side region of the shell), the same thickness
326 change affects the whole height of the tablet, resulting in a smaller relative deformation and then to a
327 less dense and stiff compact in this location than in the layers over the core. This effect is more
328 pronounced when the layer is thin. As a consequence, the pressure on the core increases when the
329 thickness of the layer decreases, explaining the higher deformations of the core with a thin layer, as
330 seen previously (Figure 2). Moreover, the radial stress in the band (Figure 6.B) has an additive effect:
331 the highest axial stress concentration on the core corresponds to the case with the lowest radial
332 stress (Figure 6.B). Thereby, the band opposes less to the diametral extension and the core deforms
333 more easily in the radial direction.

334 4.2. Influence of the core diameter

335 The stress states in both axial and radial directions are presented in Figure 7 for the same apparent
336 pressure of 50MPa.

337 As for the layer thickness, the diameter of the core modifies the concentrated axial stress on the core
338 (Figure 7.A) which should increase the deformation of the core. However, it has an inverse effect on
339 the radial stress which is also higher for small diameter (Figure 7.B) which should decrease the core
340 deformation. Whereas the effects were additive in the case of the layer thickness, they are opposite in
341 the case of the diameter. This might explain why it was more difficult to extract a consistent trend from
342 the experimental results presented above.

343 Thereby, the particular distributions of stresses applied on the core have been highlighted, in regards
344 to the layer thickness and the core diameter. The stress distribution analysis gives a mechanical
345 interpretation to the cause of the core deformations, but it also raises the interest on the shell
346 heterogeneity, which will be studied in the following section.

347 4.3. Density distribution in the shell

348 As well as the stresses, the density in the shell is not homogeneous, as it has been observed visually
349 (Ascani et al., 2019) and with X-ray micro-computed tomography (Nguyen et al., 2020). Regarding
350 these results, the regions of the shell that are denser are those that underwent the highest relative
351 deformation: the layers above the core. The distribution of densities in the shell can be extracted from
352 the numerical simulations and is presented in Figure 8.

353 These simulations are in full agreement with the previous observations in the literature and with the
354 results of the present work. In all cases, the band is less dense than the layers, and the stress
355 distributions correlate well with the density field in the shell. Indeed, the denser regions are stiffer and
356 are submitted to higher stresses than the less dense ones.

357 The density distribution in the band also makes it possible to validate the interpretation presented
358 above for the core deformation. Considering the layer thickness, a small thickness, which
359 corresponds to a high applied stress, also corresponds to a small density of the band, which will less
360 resist to the core deformation. The two effects are thus additive. Considering the diameter, the
361 smallest diameter, which corresponds to the highest axial stress on the core, also corresponds to the
362 highest band density which will add resistance against the core deformation. The two effects are thus
363 opposite in this case, and the trends are more complicated to extract.

364 In order to have an experimental confirmation of the simulation, it is possible to observe
365 experimentally the density heterogeneity on the surface of press-coated tablets. Scanning Electron

366 Microscopy (SEM) was used (TM3000, Hitachi, Tokyo, Japan) on a press-coated tablet with a MCC
367 core of 8mm diameter and layer thickness of 1.0mm, compacted at a 50MPa apparent pressure, to
368 observe its surface porosity. The output images are shown on Figure 9.

369 Both images are taken on the exact same tablet, but on regions with different densities in the
370 simulations results: the band surface (Figure 9.A) and the layer surface (Figure 9.B). This observation
371 confirms the high density gradient from the simulations results: the layer above the core is much
372 denser than the band.

373 4.4. Consequences

374 The results presented above give new insights in the understanding of the compression of press-
375 coated tablets.

376 The first important result presented above is that, even at very low apparent pressure, the final
377 compression step promotes a significant change in the structure of the core, in terms of
378 density/porosity and mechanical strength. It is well-known that these parameters play a key role in the
379 final release profile of a tablet. As a consequence, as its structure is largely modified, the release
380 profile of the core after press-coating might be very different from the release profile of the original
381 core. This is an important result that should be taken into account during the development and
382 process parameters definition. Moreover, the geometrical features of the final form, i.e. layer
383 thickness and core diameter, have both an influence on the final properties of the core. As a
384 consequence, they might also influence the final release profile of the core.

385 Of course, the release profile of a core-coated tablet is also largely influenced by the properties of the
386 shell, in terms of density and mechanical resistance. These two parameters are of course influenced
387 by the apparent pressure used for the final compression step. Nevertheless, as shown in Figure 9, the
388 density in the shell is also largely influenced by the thickness of the upper and lower layers and by the
389 ratio between the diameter of the core and the diameter of the final tablet. These two parameters
390 have then again an influence on the final release profile of the press-coated tablet. They should thus
391 be considered as critical parameters during the design and development of a press-coated tablet.

392 The second point we would like to emphasize is related to a more fundamental understanding of the
393 compression of powders. It is usual to characterize the compaction behavior of a powder using the
394 compactibility, i.e. the tensile strength of a tablet as a function of the density (or porosity). There is in

395 fact no strict bijection between density and tensile strength, i.e. it is possible to obtain different tensile
396 strengths for the same porosity, if the compression path is different. This phenomenon is often called
397 “path dependence” in the literature and has been demonstrated for various powders (Galen and
398 Zavaliangos, 2005; Koerner, 1978). Usually, this phenomenon is demonstrated using triaxial
399 compression. The case of core coating is another interesting example of the path dependence.
400 Indeed, the triaxiality of the stress on the core is not the same as the one during close die
401 compaction. As a consequence, the relation between the strength of the core and its density is not the
402 same as in normal die compaction as it can be seen in Figures 3 and 5. Moreover, it can be easily
403 foreseen that the triaxiality of the stress on the core depends on the mechanical properties of the
404 powder used in the shell. This was already used in the past in a paper (Carstensen et al., 1985)
405 where the authors used core-coating technique with a shell composed of small polymer beads in
406 order to obtain a different triaxiality to avoid capping. So, as the mechanical properties of the shell
407 might influence the stress triaxiality on the core during the final compression, they will also influence
408 the final state of the core (density, strength) and, as a consequence, its release profile. This is
409 important to consider during the development of a press-coated tablet.

410 **5. Conclusion**

411 In this study, it has been highlighted that, during coating-compression, the structure of the core is
412 modified both in terms of density and of mechanical strength. This occurs even if the final apparent
413 pressure used is much lower than the pressure used to manufacture the core. Due to stress
414 concentration phenomena that are peculiar to this type of compression, the physical state of the core
415 is highly modified along the compression process. It has been shown that the layer thickness and the
416 core-shell diameter ratio are critical parameters that influence the stress distribution and triaxiality that
417 are specific to the press-coating. The dimensions and mechanical properties of the core after the
418 coating-compression are thus strongly dependent on these parameters. Both shall thus be considered
419 as critical process parameters and be taken in account in the design of press-coated tablet to reach
420 the aimed quality attributes.

421 **Legend to figures**

422 **Figure 1:** Schematic cross section view of a press-coated tablet, and region names used in the study

423 **Figure 2:** Dimension and density variation of the MCC (A,B,C) and Lactose (D,E,F) cores versus
424 coating-compression pressure for different layer thicknesses: Core diameter (A,D) Core thickness
425 (B,E) Core density (C,F)

426 **Figure 3:** Tensile strength of the MCC (A,B) and Lactose (C,D) cores after compression depending
427 on the apparent pressure (A,C) and on their density (B,D)

428 **Figure 4:** Dimensions and density relative variations of different sizes of cores of MCC (A,B,C) and
429 Lactose (D,E,F) after coating-compression: Core diameter (A,D) ; Core thickness (B,E) ; Density (C,F)

430 **Figure 5:** Tensile strength of the cores of different diameters after compression depending on the
431 apparent compression-pressure (A,C) and on the core density (B,D)

432 **Figure 6:** Simulated axial stress (A) and radial stress (B) fields at an apparent axial pressure of
433 50MPa obtained with different layer thicknesses of 0.6mm (i) 1.0mm (ii) and 1.8mm (iii)

434 **Figure 7:** Simulated axial stress (A) and radial stress (B) fields at an apparent axial pressure of
435 50MPa obtained with different core diameters of 6mm (i) 8mm (ii) and 11.28mm (iii)

436 **Figure 8:** Simulated relative density field at an apparent compression pressure of 50MPa with
437 different layer thicknesses (A) of 0.6mm (i) 1.0mm (ii) and 1.8mm (iii) and with different core
438 diameters (B) of 6mm (i) 8mm (ii) and 11.28mm (iii)

439 **Figure 9:** SEM images of the surface of a press-coated tablet (MCC core and MCC shell; 8mm core
440 diameter; 1.0mm thickness; 50MPa apparent compression pressure) upon the center region (A) and
441 on the band region (B)

442 **Legend to tables**

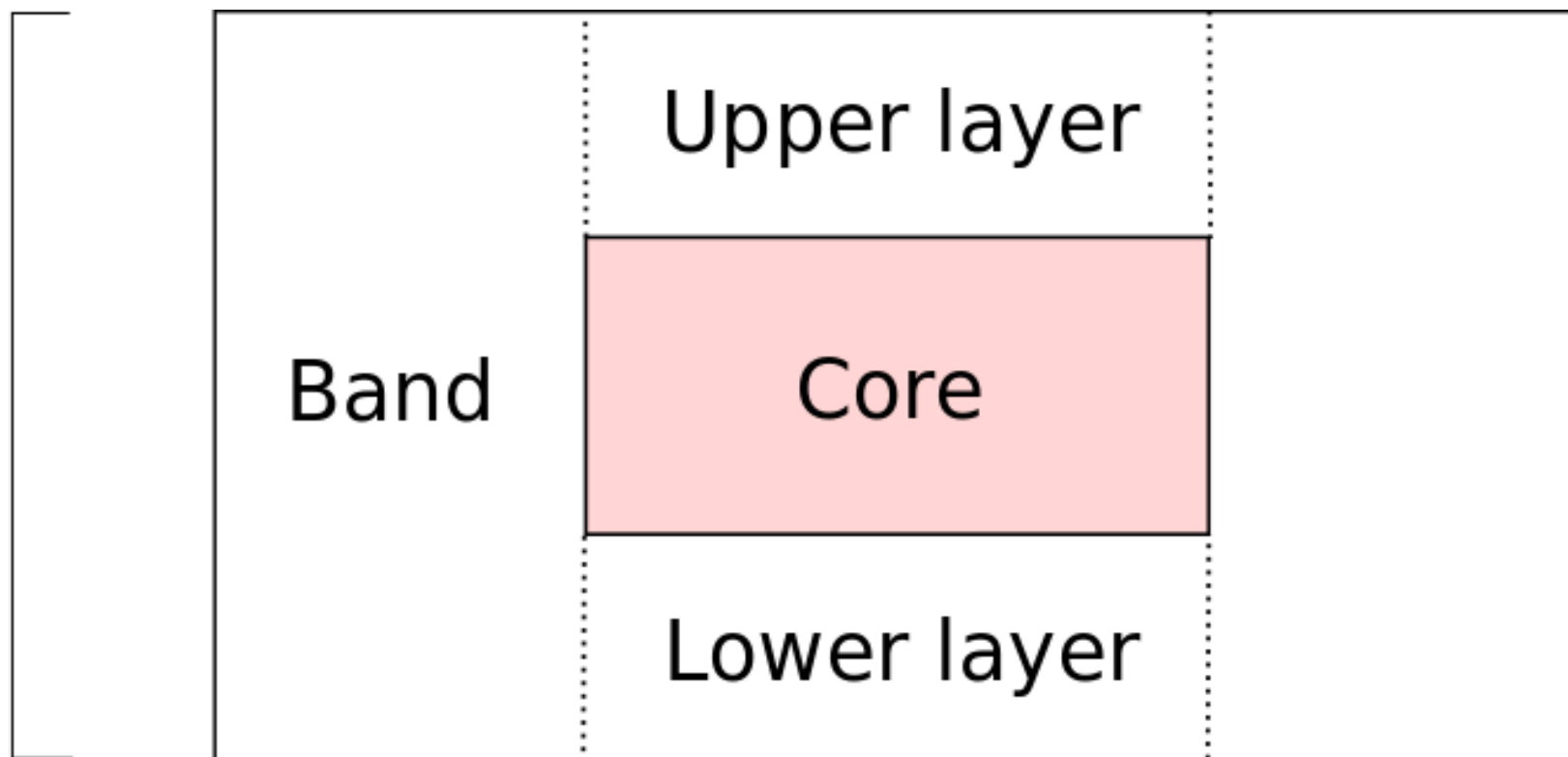
443 **Table 1:** Manufacturing parameters of the cores

444 **References**

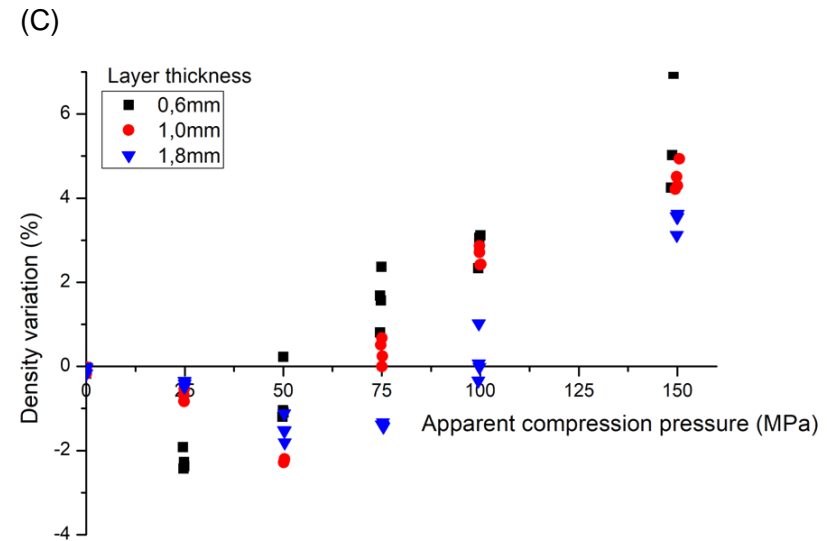
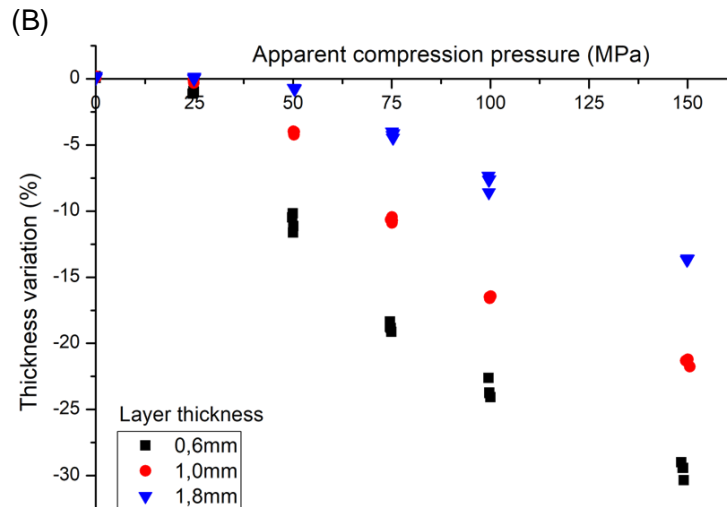
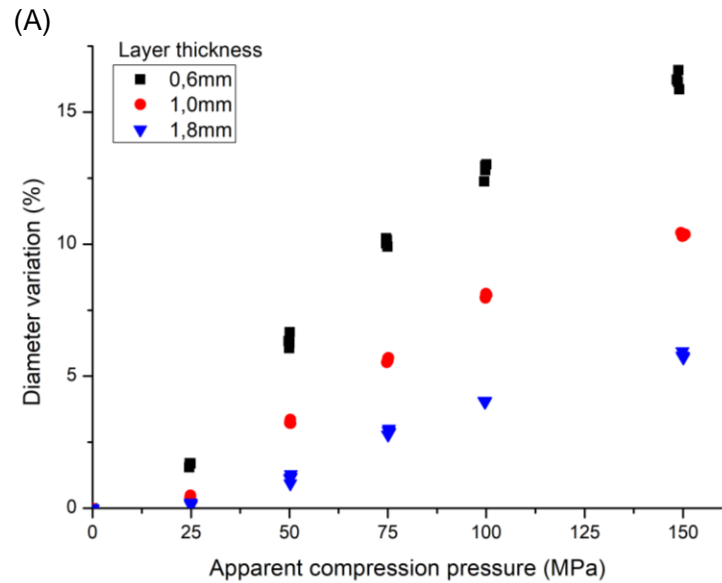
- 445 Ascani, S., Berardi, A., Bisharat, L., Bonacucina, G., Cespi, M., Palmieri, G.F., 2019. The influence of
446 core tablets rheology on the mechanical properties of press-coated tablets. *Eur. J. Pharm. Sci.*
447 135, 68–76. <https://doi.org/10.1016/j.ejps.2019.05.011>
- 448 Carstensen, J.T., Alcorn, G.J., Hussain, S.A., Zoglio, M.A., 1985. Triaxial Compression of “Cappable”
449 Formulations. *J. Pharm. Sci.* 74, 1239–1241. <https://doi.org/10.1002/jps.2600741121>
- 450 Conte, U., Maggi, L., Torre, M.L., Giunchedi, P., Manna, A.L., 1993. Press-coated tablets for time-
451 programmed release of drugs. *Biomaterials* 14, 1017–1023. [https://doi.org/10.1016/0142-9612\(93\)90195-8](https://doi.org/10.1016/0142-9612(93)90195-8)
- 452
- 453 Cunningham, J.C., Sinka, I.C., Zavaliangos, A., 2004. Analysis of tablet compaction. I.
454 Characterization of mechanical behavior of powder and powder/tooling friction. *J. Pharm. Sci.*
455 93, 2022–2039. <https://doi.org/10.1002/Jps.20110>

- 456 Diarra, H., Mazel, V., Boillon, A., Rehault, L., Busignies, V., Bureau, S., Tchoreloff, P., 2012. Finite
457 Element Method (FEM) modeling of the powder compaction of cosmetic products: Comparison
458 between simulated and experimental results. *Powder Technol.* 224, 233–240.
459 <https://doi.org/10.1016/j.powtec.2012.02.058>
- 460 Diarra, H., Mazel, V., Busignies, V., Tchoreloff, P., 2013. FEM simulation of the die compaction of
461 pharmaceutical products: Influence of visco-elastic phenomena and comparison with
462 experiments. *Int. J. Pharm.* 453, 389–394. <https://doi.org/10.1016/j.ijpharm.2013.05.038>
- 463 Fell, J.T., Newton, J.M., 1970. Determination of Tablet Strength by the Diametral-Compression Test.
464 *J. Pharm. Sci.* 59, 688–691. <https://doi.org/10.1002/jps.2600590523>
- 465 Foppoli, A.A., Maroni, A., Cerea, M., Zema, L., Gazzaniga, A., 2017. Dry coating of solid dosage
466 forms: an overview of processes and applications. *Drug Dev. Ind. Pharm.* 43, 1919–1931.
467 <https://doi.org/10.1080/03639045.2017.1355923>
- 468 Fukui, E., Uemura, K., Kobayashi, M., 2000. Studies on applicability of press-coated tablets using
469 hydroxypropylcellulose (HPC) in the outer shell for timed-release preparations. *J. Controlled
470 Release* 68, 215–223. [https://doi.org/10.1016/S0168-3659\(00\)00261-3](https://doi.org/10.1016/S0168-3659(00)00261-3)
- 471 Galen, S., Zavaliangos, A., 2005. Strength anisotropy in cold compacted ductile and brittle powders.
472 *Acta Mater.* 53, 4801–4815. <https://doi.org/10.1016/j.actamat.2005.06.023>
- 473 Gandhi, B.R., Mundada, A.S., Gandhi, P.P., 2011. Chronopharmaceutics: As a clinically relevant drug
474 delivery system. *Drug Deliv.* 18, 1–18. <https://doi.org/10.3109/10717544.2010.509358>
- 475 Jagdale, S.C., Suryawanshi, V.M., Pandya, S.V., Kuchekar, B.S., Chabukswar, A.R., 2014.
476 Development of Press-Coated, Floating-Pulsatile Drug Delivery of Lisinopril. *Sci. Pharm.* 82,
477 423–440. <https://doi.org/10.3797/scipharm.1301-27>
- 478 Kaljević, O., Djuriš, J., Djurić, Z., Ibrić, S., 2016. Application of failure mode and effects analysis in
479 quality by design approach for formulation of carvedilol compression coated tablets. *J. Drug
480 Deliv. Sci. Technol.* 32, 56–63. <https://doi.org/10.1016/j.jddst.2016.02.004>
- 481 Koerner, R.M., 1978. Triaxial Stress State Compaction of Powders, in: *Powder Metallurgy Processing*.
482 Elsevier, pp. 33–50. <https://doi.org/10.1016/B978-0-12-428450-0.50008-2>
- 483 Lin, S.-Y., Kawashima, Y., 2012. Current status and approaches to developing press-coated
484 chronodelivery drug systems. *J. Controlled Release* 157, 331–353.
485 <https://doi.org/10.1016/j.jconrel.2011.09.065>
- 486 Maity, S., Sa, B., 2016. Compression-Coated Tablet for Colon Targeting: Impact of Coating and Core
487 Materials on Drug Release. *AAPS PharmSciTech* 17, 504–515.
488 <https://doi.org/10.1208/s12249-015-0359-0>
- 489 Mazel, V., Diarra, H., Busignies, V., Tchoreloff, P., 2014. Comparison of different failure tests for
490 pharmaceutical tablets: Applicability of the Drucker–Prager failure criterion. *Int. J. Pharm.* 470,
491 63–69. <https://doi.org/10.1016/j.ijpharm.2014.05.006>
- 492 Nguyen, T.-T., Park, H.-R., Cho, C.-H., Hwang, K.-M., Park, E.-S., 2020. Investigation of critical
493 factors affecting mechanical characteristics of press-coated tablets using a compaction
494 simulator. *Int. J. Pharm.* 582, 119308. <https://doi.org/10.1016/j.ijpharm.2020.119308>
- 495 Roberts, R.J., Rowe, R.C., 1987. The compaction of pharmaceutical and other model materials - a
496 pragmatic approach. *Chem. Eng. Sci.* 42, 903–911. [https://doi.org/10.1016/0009-2509\(87\)80048-9](https://doi.org/10.1016/0009-2509(87)80048-9)
- 498 Sawada, T., Kondo, H., Nakashima, H., Sako, K., Hayashi, M., 2004. Time-release compression-
499 coated core tablet containing nifedipine for chronopharmacotherapy. *Int. J. Pharm.* 280, 103–
500 111. <https://doi.org/10.1016/j.ijpharm.2004.05.004>
- 501 Sinka, I. c., Cunningham, J. c., Zavaliangos, A., 2004. Analysis of tablet compaction. II. Finite element
502 analysis of density distributions in convex tablets. *J. Pharm. Sci.* 93, 2040–2053.
- 503 Tye, C.K., Sun, C. (Calvin), Amidon, G.E., 2005. Evaluation of the effects of tableting speed on the
504 relationships between compaction pressure, tablet tensile strength, and tablet solid fraction. *J.
505 Pharm. Sci.* 94, 465–472. <https://doi.org/10.1002/jps.20262>
- 506 Wu, B., Shun, N., Wei, X., Wu, W., 2007. Characterization of 5-Fluorouracil Release from
507 Hydroxypropylmethylcellulose Compression-Coated Tablets. *Pharm. Dev. Technol.* 12, 203–
508 210. <https://doi.org/10.1080/10837450601168722>
- 509 Wu, C.-Y., Ruddy, O.M., Bentham, A.C., Hancock, B.C., Best, S.M., Elliott, J.A., 2005. Modelling the
510 mechanical behaviour of pharmaceutical powders during compaction. *Powder Technol.* 152,
511 107–117. <https://doi.org/10.1016/j.powtec.2005.01.010>

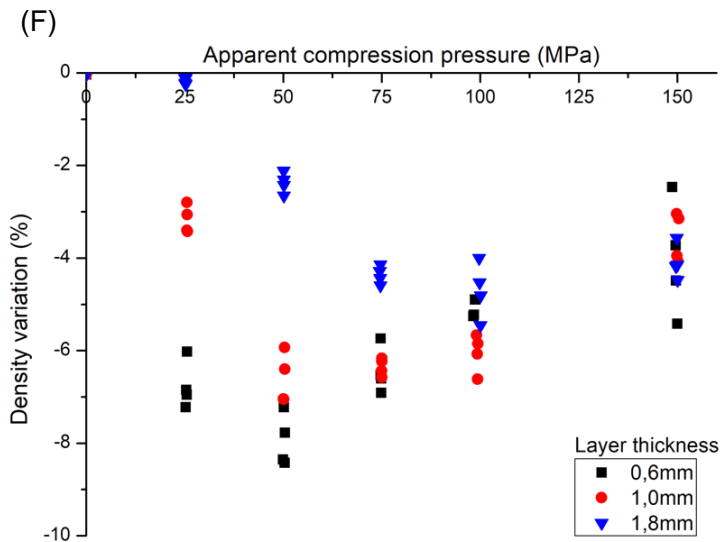
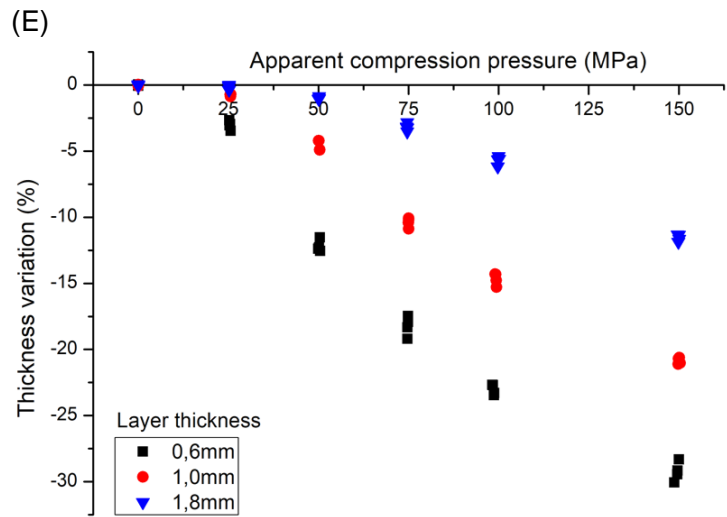
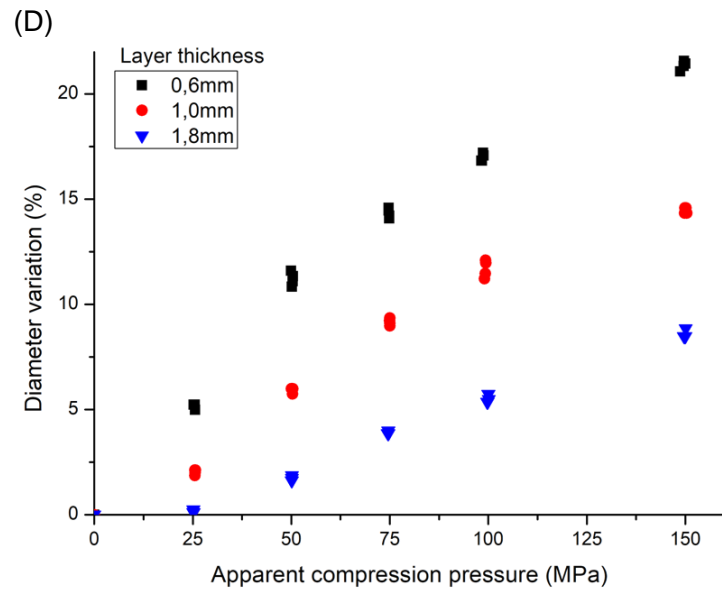
Shell =
layers + band



MCC

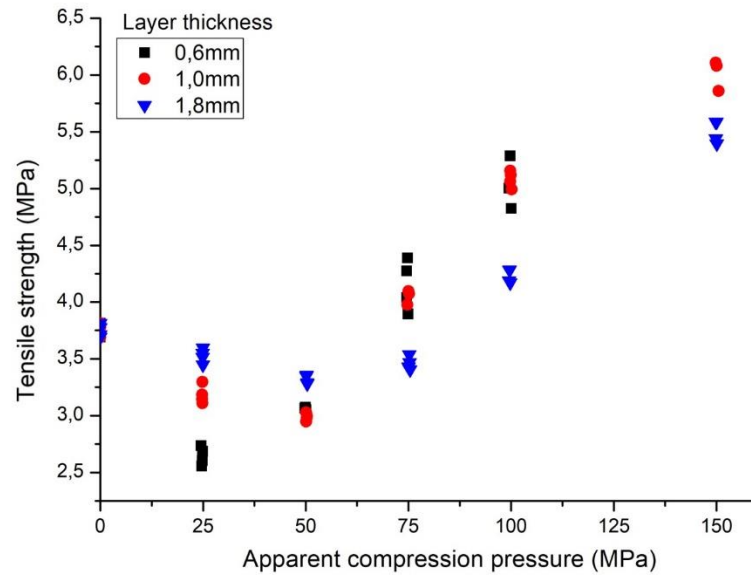


Lactose

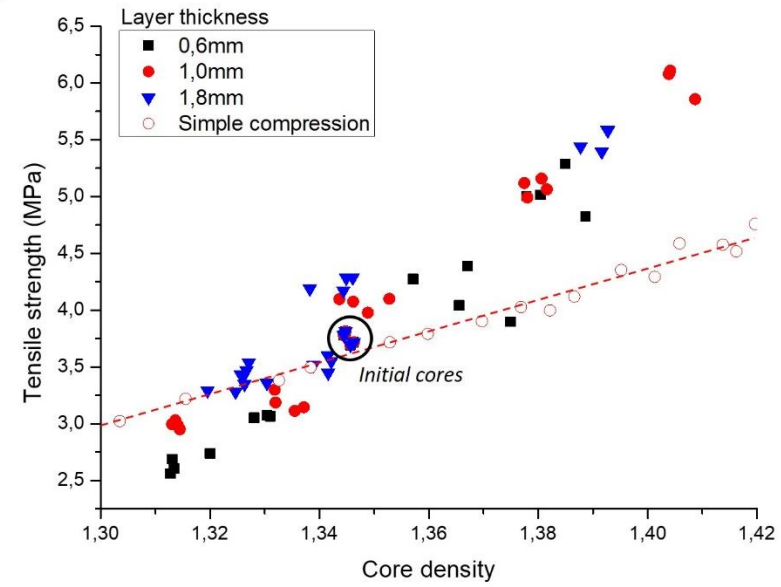


MCC

(A)

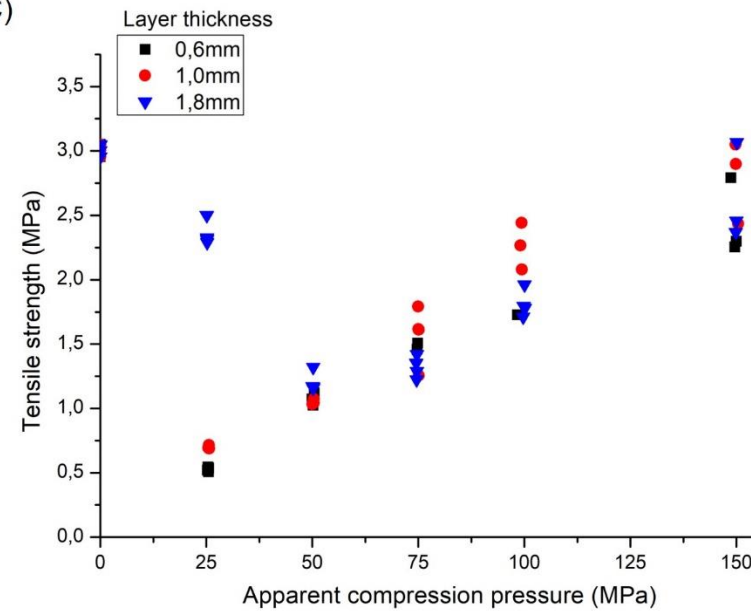


(B)

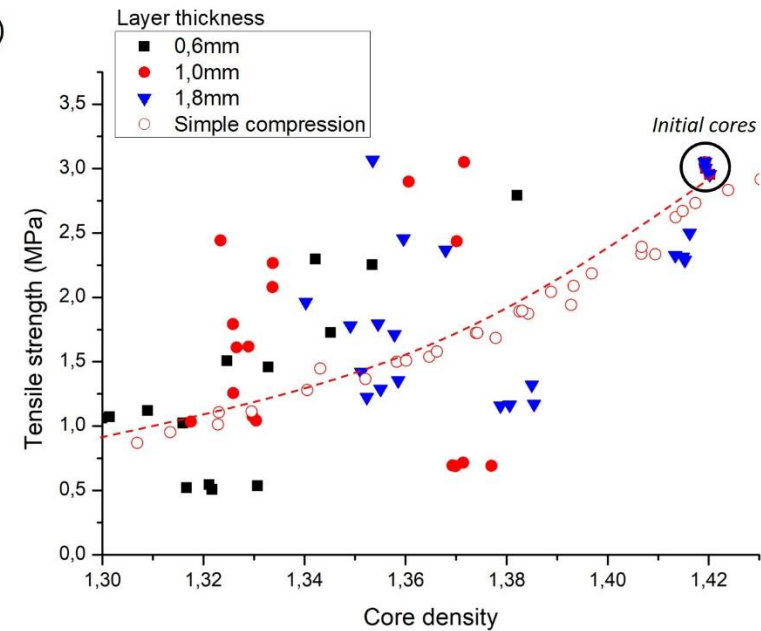


Lactose

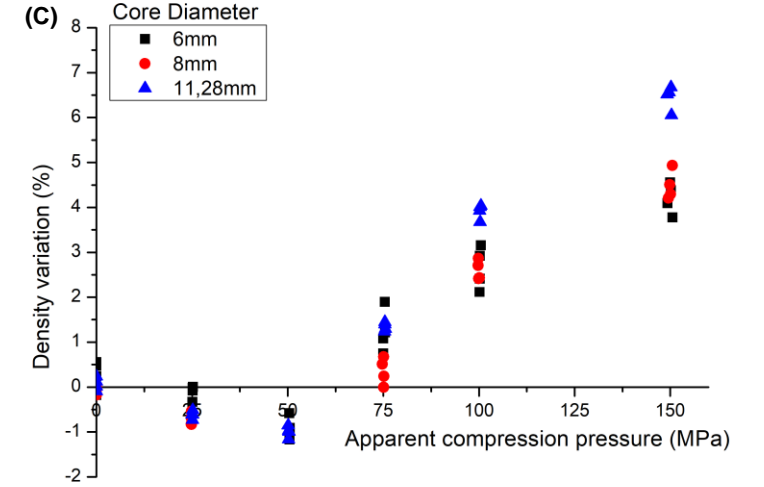
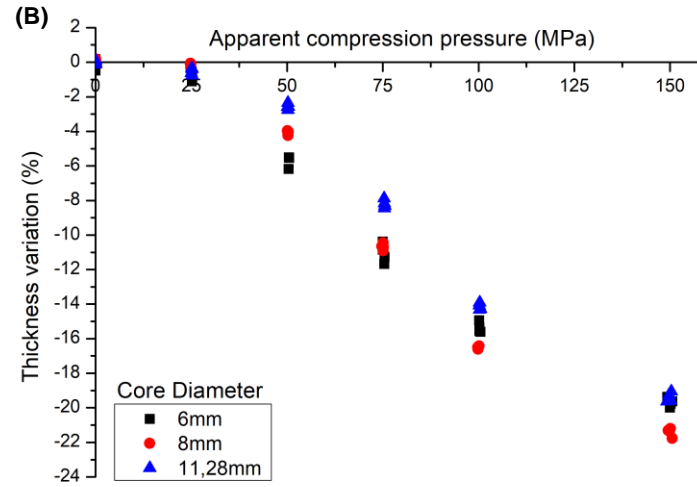
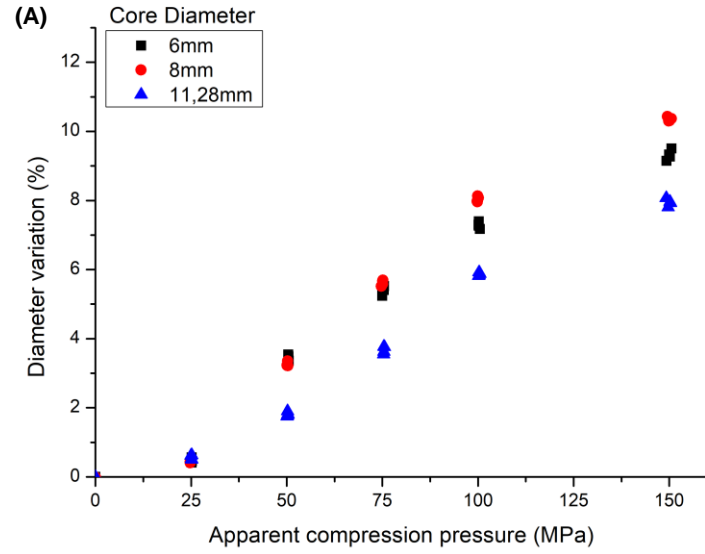
(C)



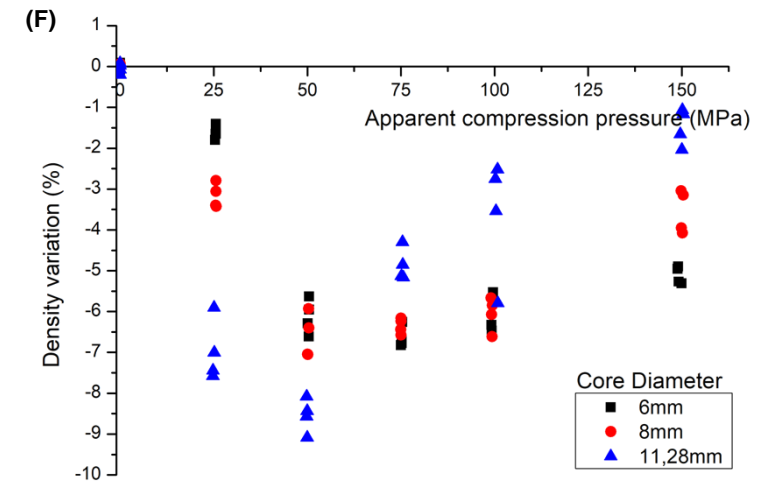
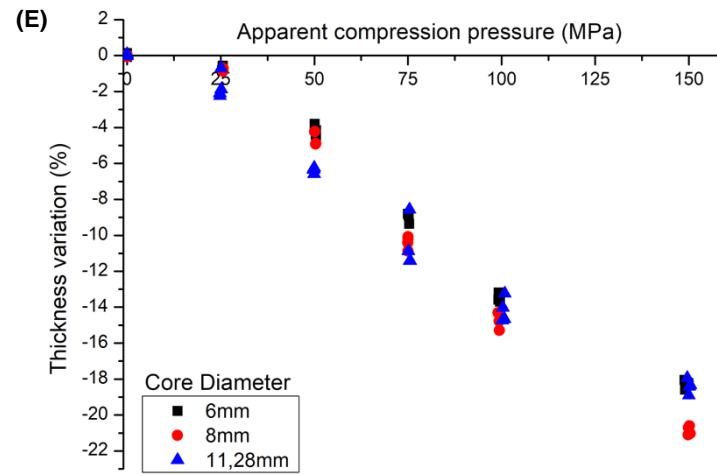
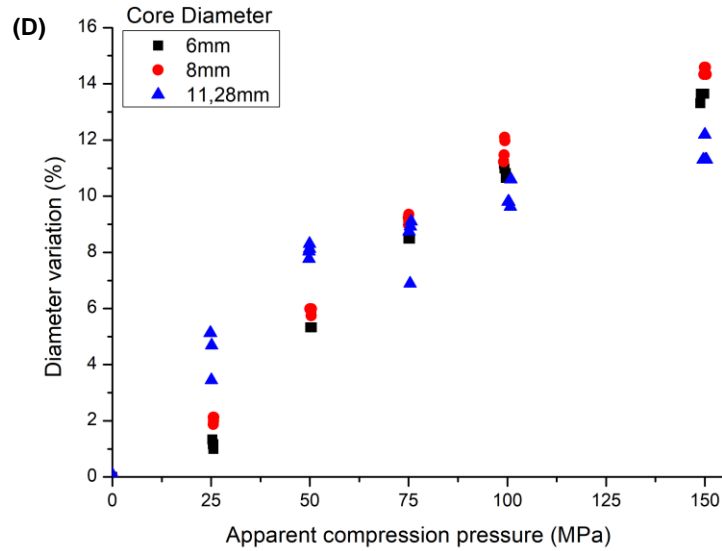
(D)



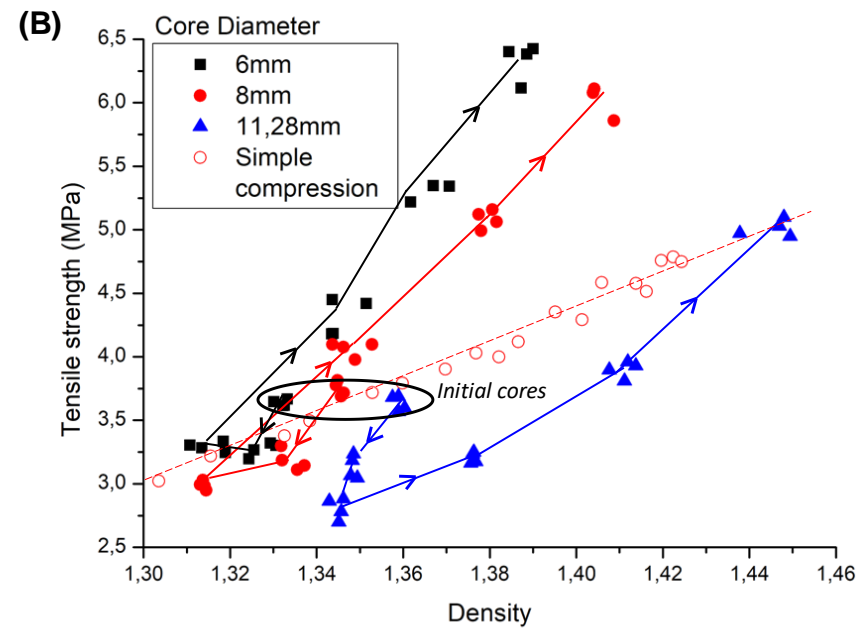
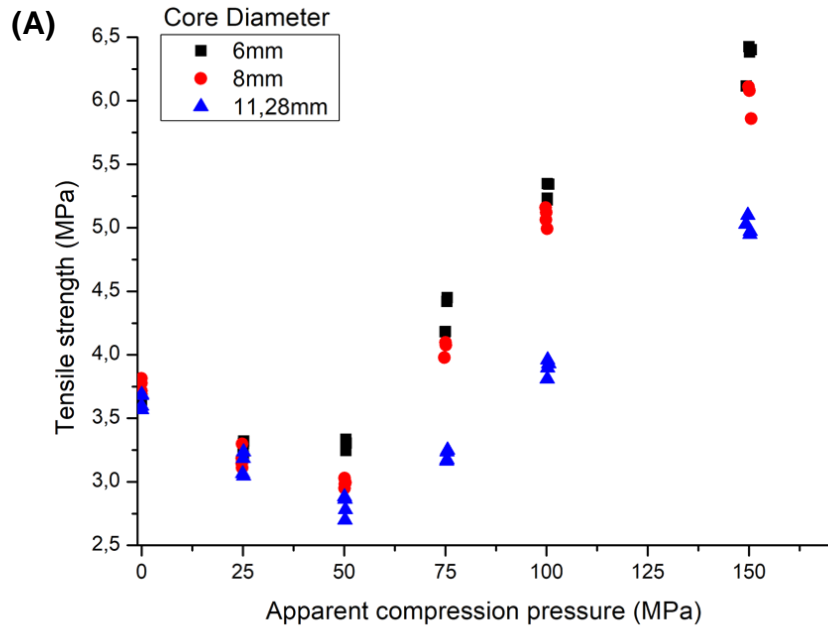
MCC



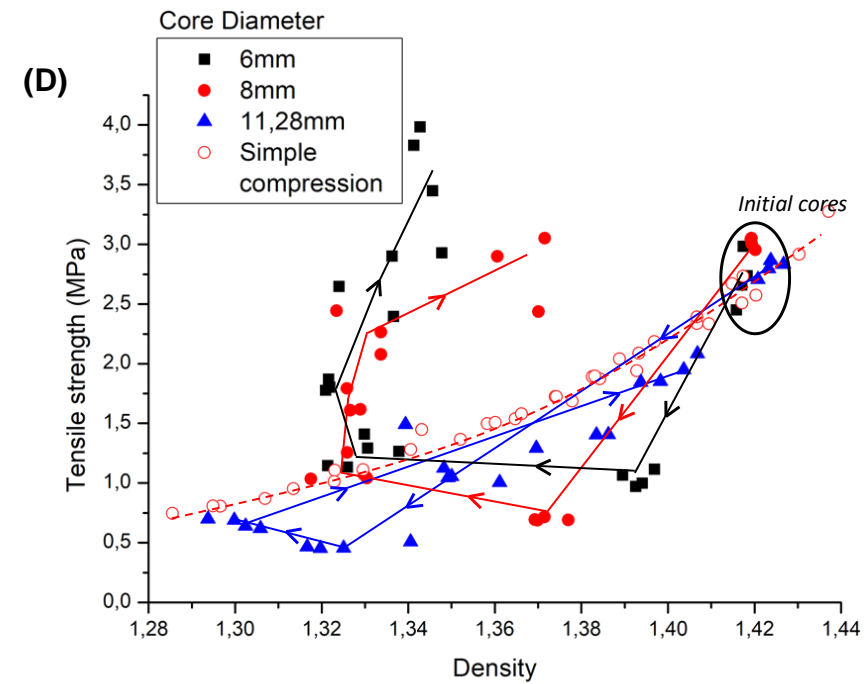
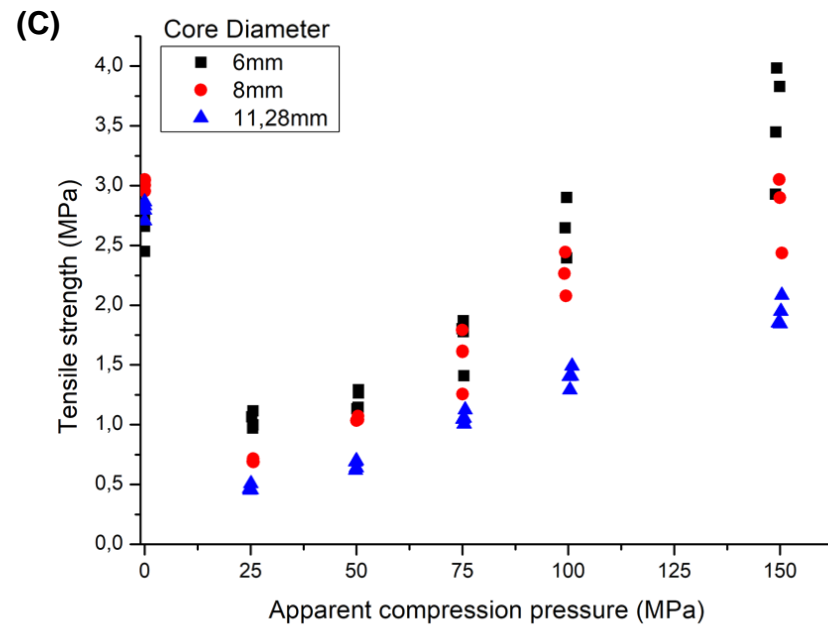
Lactose

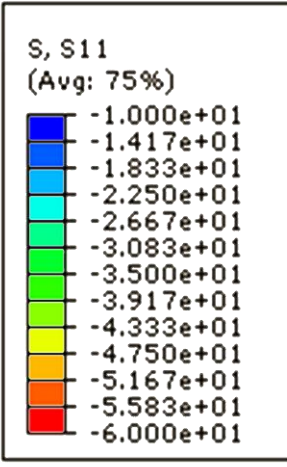
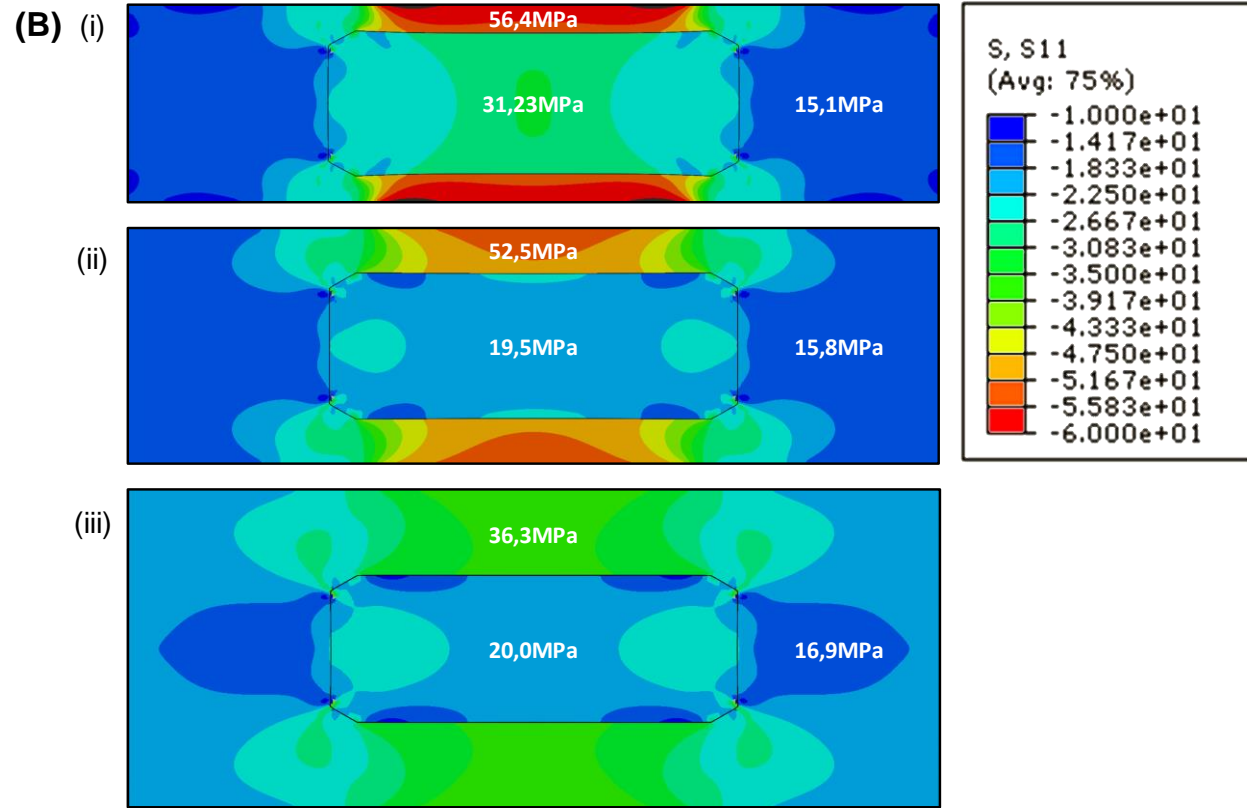
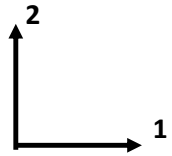
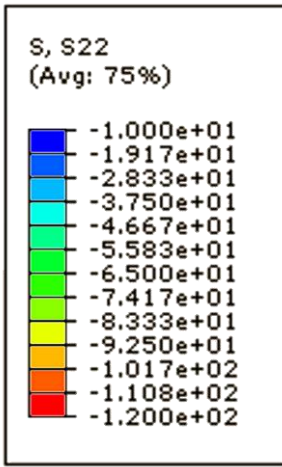
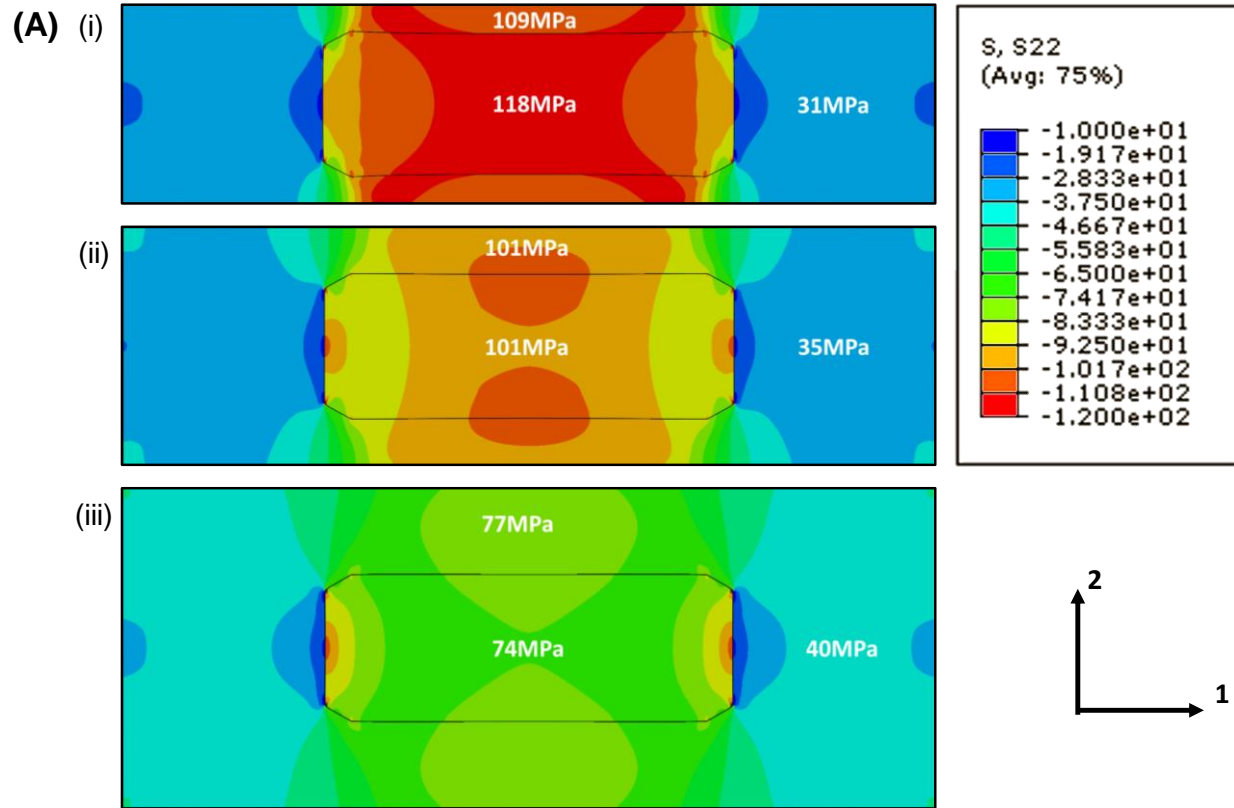


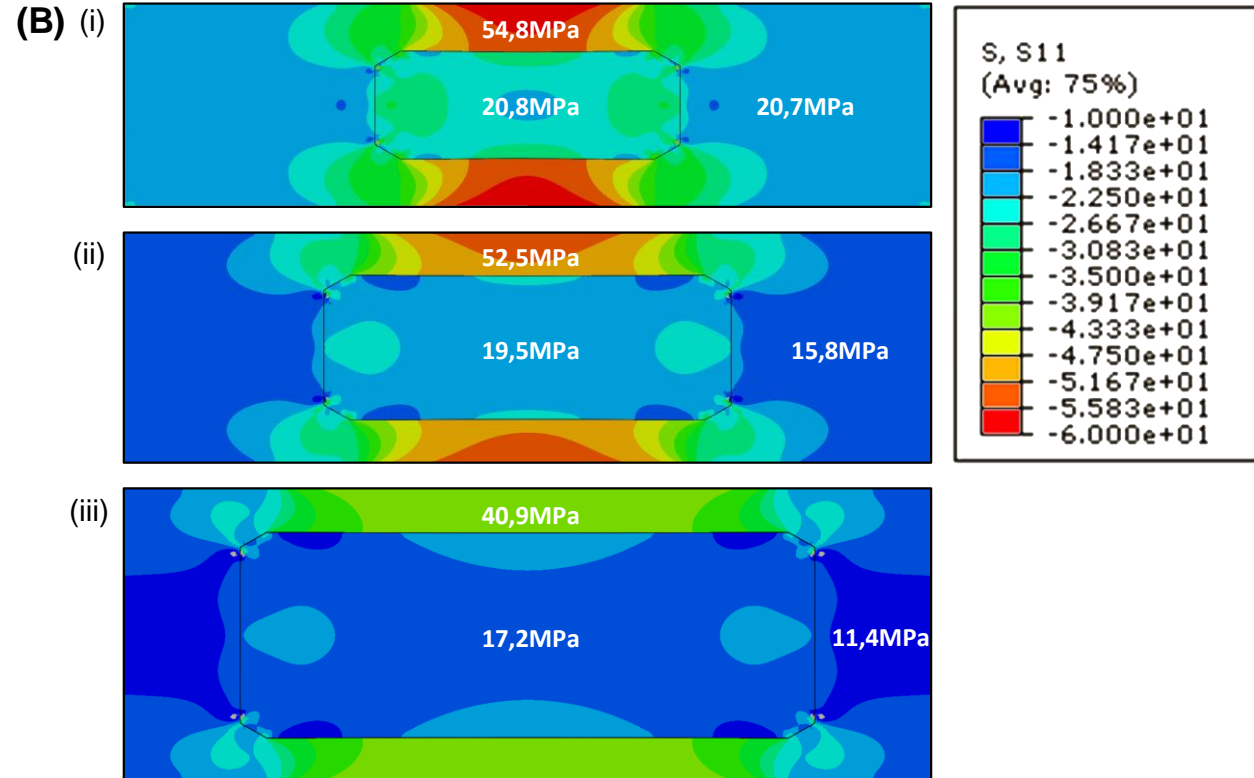
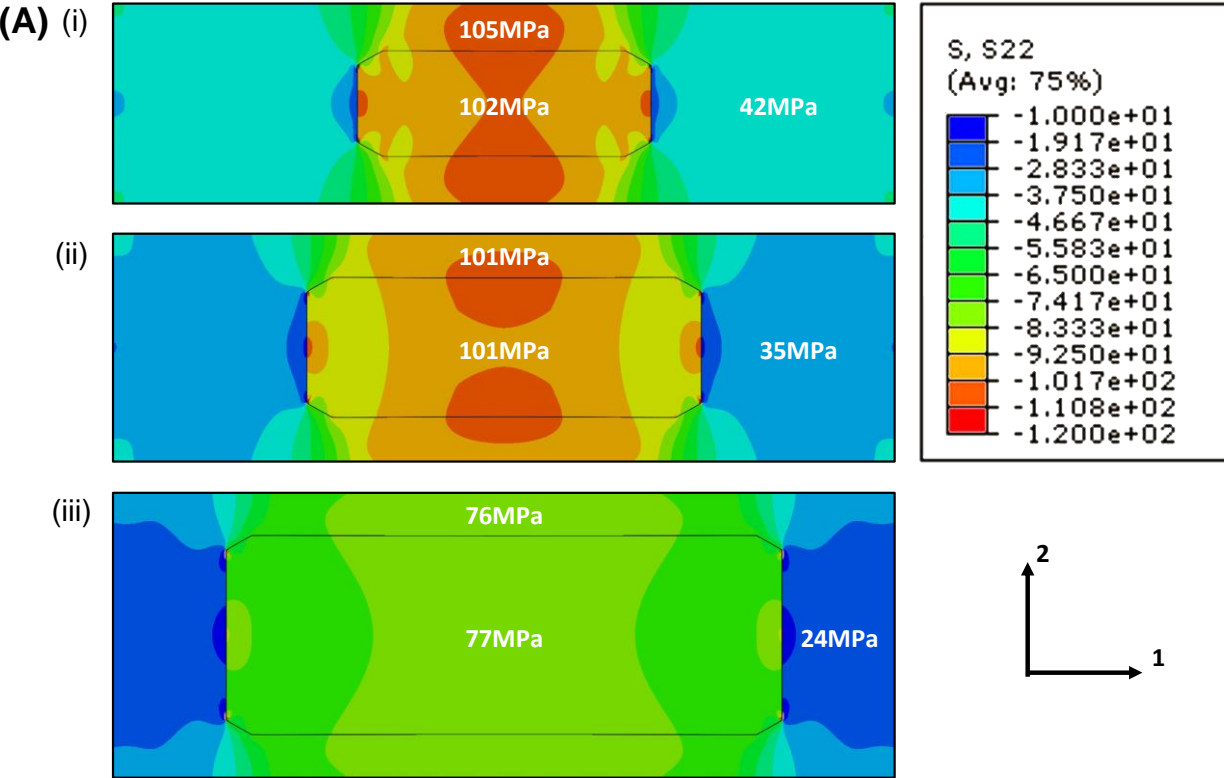
MCC

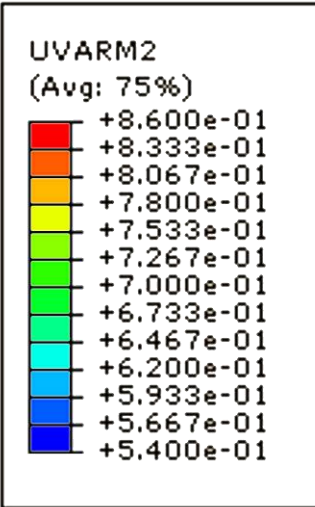
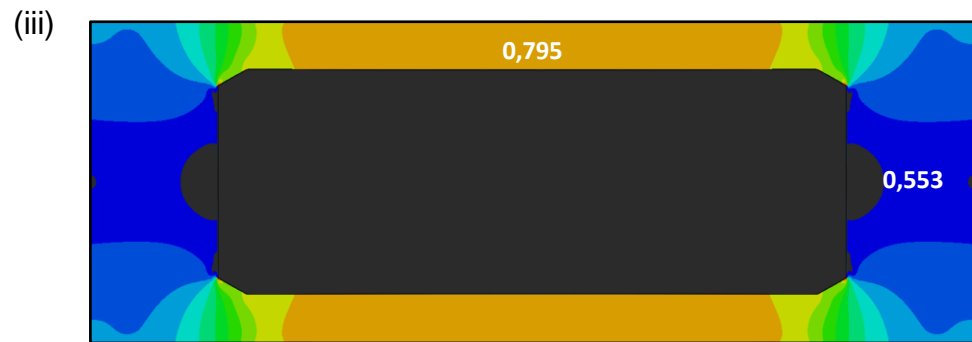
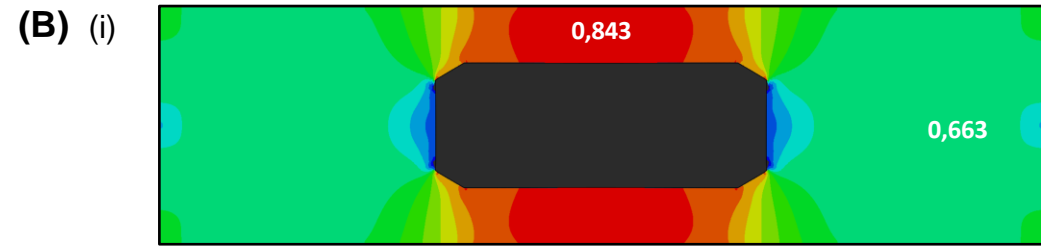
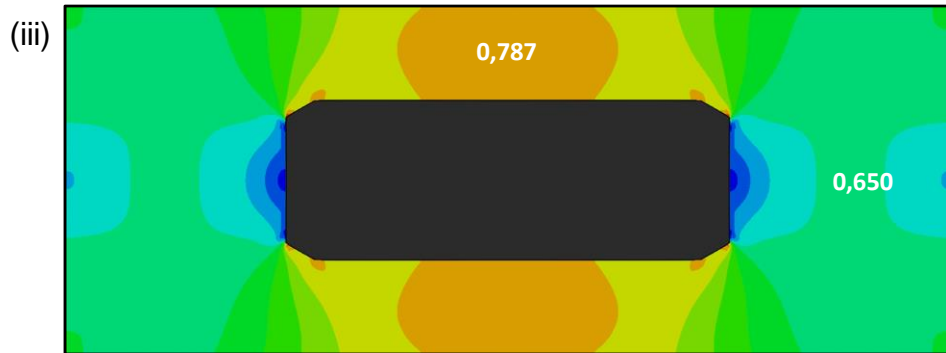
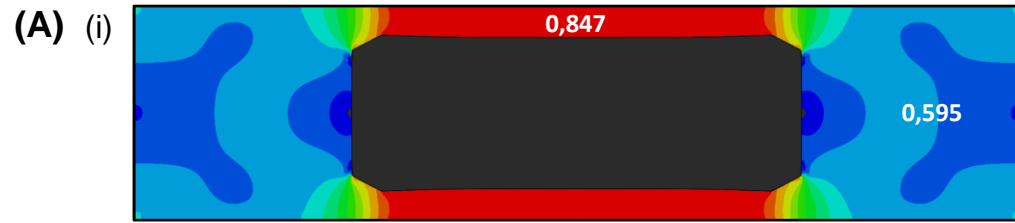


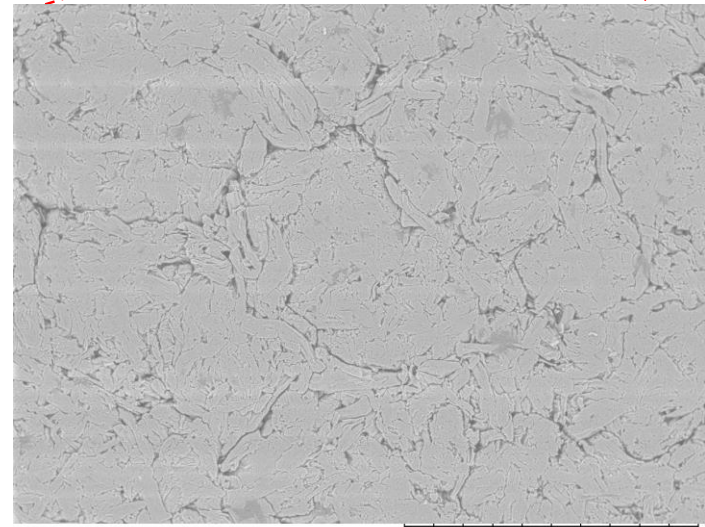
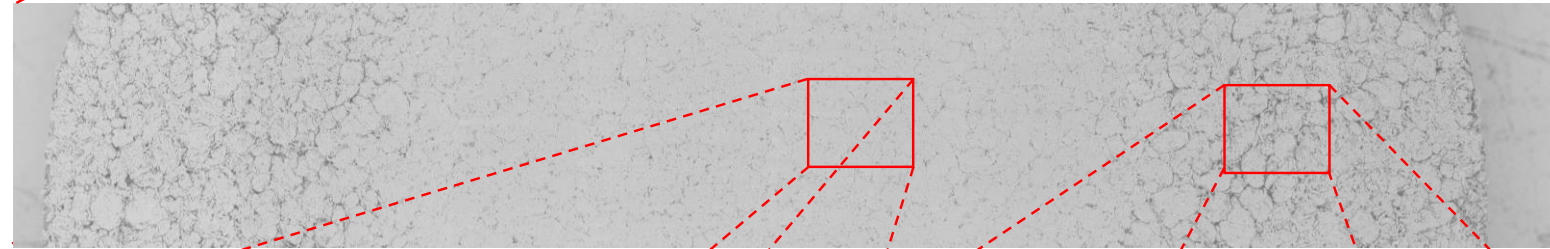
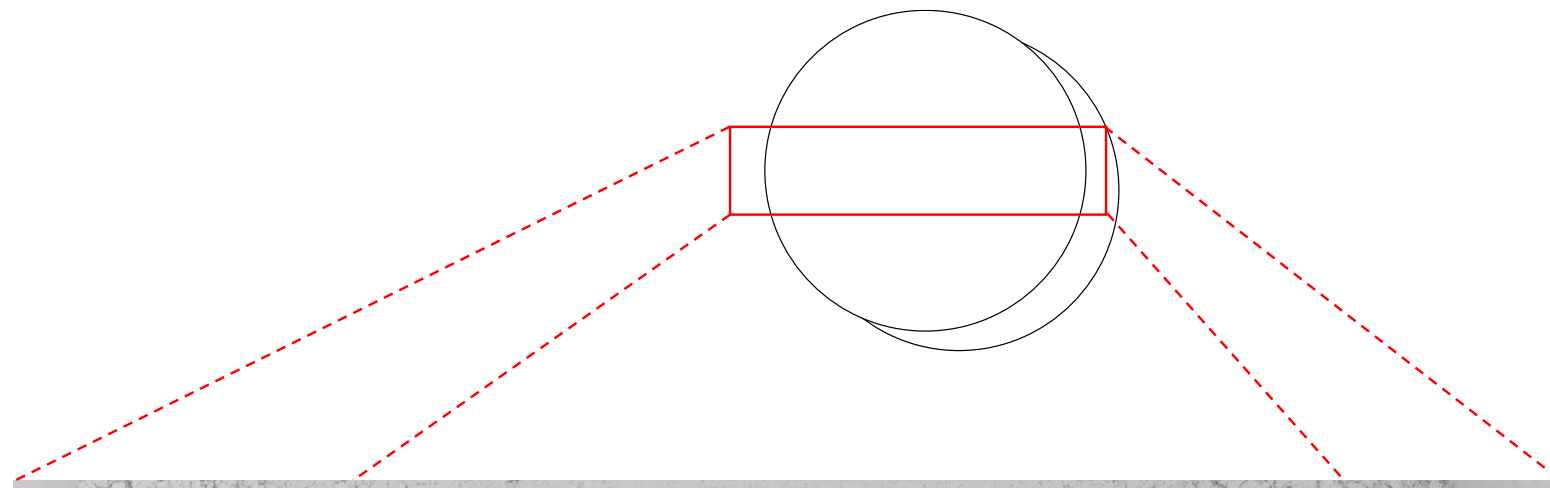
Lactose



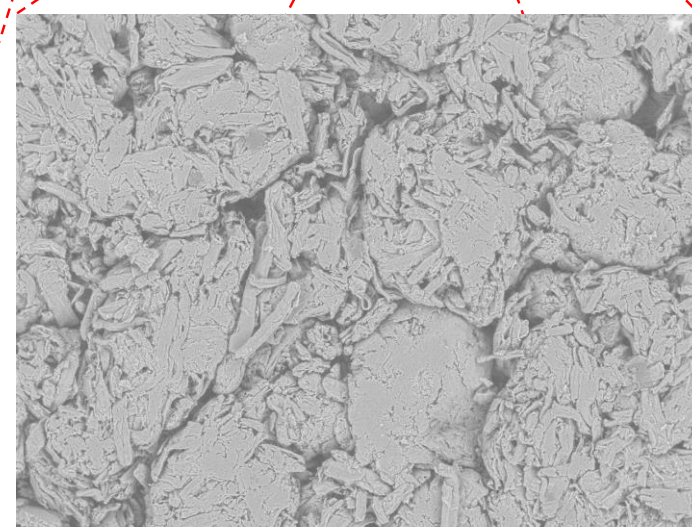








(A)



(B)

Core diameter (mm)	Core thickness (mm)	Target compression force on MCC (kN)	Equivalent pressure (MPa)	Target compression force on Lactose (kN)	Equivalent pressure (MPa)
6	2.25	4.2	150	8.4	300
8	3.00	7.5	150	15.0	300
11.28	4.23	15.0	150	30.0	300

Table 1 - Manufacturing parameters of the cores

